The selective antagonist EPPTB reveals TAAR1-mediated regulatory mechanisms in dopaminergic neurons of the mesolimbic system

Amyaouch Bradaia[a,b], Gerhard Trube[c], Henri Stalder[c], Roger D. Norcross[c], Laurence Ozmen[c], Joseph G. Wettstein[c], Audrée Pinard[a], Danièle Buchy[c], Martin Gassmann[a], Marius C. Hoener[c], and Bernhard Bettler[a,1]

[a]Department of Biomedicine, Institute of Physiology, Pharmazentrum, University of Basel, CH-4056 Basel, Switzerland; [b]Neuroservice, 13593 Aix en Provence, Cedex 03, France; and [c]Pharmaceuticals Division, Neuroscience Research, F. Hoffmann-La Roche Ltd., CH-4070 Basel, Switzerland

Edited by Shigetada Nakanishi, Osaka Bioscience Institute, Osaka, Japan, and approved September 29, 2009 (received for review June 11, 2009)

Trace amine-associated receptor 1 (TAAR1) is a G protein-coupled receptor (GPCR) that is nonselectively activated by endogenous metabolites of amino acids. TAAR1 is considered a promising drug target for the treatment of psychiatric and neurodegenerative disorders. However, no selective ligand to identify TAAR1-specific signaling mechanisms is available yet. Here we report a selective TAAR1 antagonist, EPPTB, and characterize its physiological effects at dopamine (DA) neurons of the ventral tegmental area (VTA). We show that EPPTB prevents the reduction of the firing frequency of DA neurons induced by *p*-tyramine (*p*-tyr), a nonselective TAAR1 agonist. When applied alone, EPPTB increases the firing frequency of DA neurons, suggesting that TAAR1 either exhibits constitutive activity or is tonically activated by ambient levels of endogenous agonist(s). We further show that EPPTB blocks the TAAR1-mediated activation of an inwardly rectifying K^+ current. When applied alone, EPPTB induces an apparent inward current, suggesting the closure of tonically activated K^+ channels. Importantly, these EPPTB effects were absent in *Taar1* knockout mice, ruling out off-target effects. We additionally found that both the acute application of EPPTB and the constitutive genetic lack of TAAR1 increase the potency of DA at D2 receptors in DA neurons. In summary, our data support that TAAR1 tonically activates inwardly rectifying K^+ channels, which reduces the basal firing frequency of DA neurons in the VTA. We hypothesize that the EPPTB-induced increase in the potency of DA at D2 receptors is part of a homeostatic feedback mechanism compensating for the lack of inhibitory TAAR1 tone.

desensitization | dopamine supersensitivity | Kir3 | trace amines | VTA

Trace amines (TAs) such as *p*-tyr, β-phenylethylamine, octopamine, and tryptamine are metabolites of amino acids that are found at low concentrations in the brain (1). Because of their structural similarity to classical biogenic amines, TAs were for a long time believed to modulate neurotransmission by displacing biogenic amines from vesicular stores or by acting on transporters in an amphetamine-like manner. It was not until TAs were found to bind to members of a family of GPCRs, the TA-associated receptors (TAARs), that receptor-mediated mechanisms were evoked (2–5). While several TAARs were identified, only TAAR1 and, to a lesser extent, TAAR4 respond to typical TAs (5). TAs such as *p*-tyr and β-phenylethylamine activate human, mouse, and rat TAAR1 with EC_{50} values of 0.2–1.7 μM. Other TAs (octopamine, tryptamine), classical biogenic amines, and amphetamine-related psychostimulants have much reduced potency and efficacy at TAAR1.

TA binding to TAAR1 engages G_s-type G proteins that activate adenylyl cyclases (1). However, because TAs not only activate TAAR1 but also influence the activity of TAAR4, DA transporters, adrenergic, as well as serotonin receptors it was difficult to assign specific physiological functions to TAAR1 (1, 6). With the availability of *Taar1* knockout mice (7, 8) it became clear that TAAR1 can inhibit DA neurons in the VTA via a receptor-mediated pathway. The genetic absence of TAAR1 clearly increased the spontaneous firing rate of DA neurons but the underlying signaling mechanism remained unclear (7). *Taar1* knockout mice also display behavioral and neurochemical signs of DA supersensitivity, a feature thought to relate to positive symptoms of schizophrenia (8). In addition, TAs were implicated in the etiology of depression, addiction, attention-deficit/hyperactivity disorder, and Parkinson's disease (5, 9, 10). However, validation of therapeutic concepts was hampered by the lack of a ligand that specifically regulates TAAR1 activity in vivo. Here we report the identification of a selective TAAR1 antagonist, N-(3-Ethoxy-phenyl)-4-pyrrolidin-1-yl-3-trifluoromethyl-benzamide [EPPTB, CAS Registry Number 1110781–88-8, (11)], which we used to study the signaling mechanisms of TAAR1 in DA neurons of the VTA. Surprisingly, we found that TAAR1 not only tonically activates inwardly rectifying K^+ channels, but that acute blockade of TAAR1 also increases the affinity of DA at D2 receptors. We discuss the implications of our findings for DA neurotransmission and drug discovery.

Results

Identification of the TAAR1 Antagonist EPPTB. For high-throughput compound screening, we stably expressed human TAAR1 in HEK293 cells. To identify antagonists, we activated the receptor with β-phenylethylamine (1.5 μM, corresponding to the EC_{80} value) and measured the compound-mediated inhibition of cAMP accumulation. Compounds with an $IC_{50} < 3$ μM in the primary screen were optimized for their physicochemical, pharmacodynamic, and pharmacokinetic properties using medicinal chemistry. This resulted in the identification of the TAAR1 antagonist EPPTB (Fig. 1). EPPTB potently antagonized cAMP production induced by activating mouse TAAR1 with 1.5 μM β-phenylethylamine ($IC_{50} = 27.5 \pm 9.4$ nM, Fig. S1). Schild plot analysis revealed a competitive mode of action of EPPTB (Fig. S2). Interestingly, EPPTB reduced TAAR1-stimulated cAMP production in stably transfected HEK293 cells below basal levels ($-12.3 \pm 4.7\%$). This suggests that TAAR1 exhibits agonist independent constitutive activity and that EPPTB is an inverse agonist. Consistent with this notion, cAMP levels were dose-dependently reduced by EPPTB in HEK293 cells in the absence of TAAR1 agonist ($-10.2 \pm 4.5\%$, $IC_{50} = 19 \pm 12$ nM). EPPTB was significantly more potent in antagonizing cAMP production by mouse, as compared to rat ($IC_{50} = 4539 \pm 2051$ nM) and

Author contributions: A.B., M.C.H., and B.B. designed research; A.B., G.T., H.S., R.D.N., L.O., A.P., D.B., and M.C.H. performed research; A.B., G.T., A.P., and M.C.H. analyzed data; and A.B., G.T., J.G.W., M.G., M.C.H., and B.B. wrote the paper.

The authors declare no conflict of interest.

This article is a PNAS Direct Submission.

[1]To whom correspondence should be addressed. E-mail: bernhard.bettler@unibas.ch.

This article contains supporting information online at www.pnas.org/cgi/content/full/0906522106/DCSupplemental.

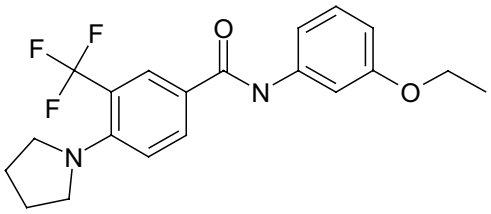

Fig. 1. Chemical structure of the selective TAAR1 antagonist N-(3-Ethoxy-phenyl)-4-pyrrolidin-1-yl-3-trifluoromethyl-benzamide (EPPTB).

human (IC_{50} = 7487 ± 2109 nM) TAAR1. In agreement with these data, the displacement of the TAAR1 radioligand [^{3}H]-rac-2-(1,2,3,4-tetrahydro-1-naphthyl)-2-imidazoline (11) at recombinant receptors revealed an approximately 10^3-fold higher EPPTB binding-affinity at the mouse as compared to the rat receptor (Table 1). In vitro pharmacological profiling assays revealed that 10 μM EPPTB inhibited radioligand binding at classical monoaminergic targets by less than 53% (Cerep; Table S1). The monoaminergic targets included DA (D1, D2S), serotonin (5-HT1A, 1B, 2A, 3, 5A, 6, 7) and adrenergic (α1, α2, β1, β2) receptors as well as DA, serotonin, and norepinephrine transporters. Considering that the K_i for EPPTB at mouse TAAR1 is 1 nM this translates into selectivity ratios >1,000. To address TAAR1-selective effects in mouse brain, we used EPPTB at a concentration of 10 nM and performed control experiments with EPPTB in *Taar1*$^{-/-}$ mice (see below).

Blocking of TAAR1 Activity Increases the Firing Frequency of DA Neurons in the VTA. We first addressed whether EPPTB inhibits the *p*-tyr-mediated inhibition of the spontaneous firing frequency of DA neurons in slice preparations of the VTA (7, 12). Bath application of EPPTB (10 nM) under current-clamp conditions not only prevented the inhibition of the firing frequency of DA neurons induced by *p*-tyr (10 μM), but significantly increased the firing frequency over the basal level (Fig. 2*A*). As a control, *p*-tyr by itself or in combination with EPPTB failed to alter the firing frequency of DA neurons in *Taar1*$^{-/-}$ mice (Fig. 2*B*). However, as reported earlier (7), the basal firing rate in *Taar1*$^{-/-}$ mice was significantly increased compared to wild-type (WT) littermate mice, suggesting that TAAR1 in DA neurons of the VTA is normally constitutively active or tonically activated by ambient levels of endogenous agonist(s). Accordingly, we found that EPPTB by itself significantly and reversibly increased the basal firing rate of DA neurons in WT but not in *Taar1*$^{-/-}$ mice (Fig. 2 *C* and *D*). Under current-clamp conditions, the *p*-tyr-induced decrease in the firing frequency of WT DA neurons was associated with a hyperpolarization of the membrane potential from −49.6 ± 0.4 to −57.6 ± 0.7 mV (n = 15), consistent with earlier findings (7, 12). Since in voltage-clamp recordings *p*-tyr application to DA neurons caused a drop in input resistance [see below and (12)], this hyperpolarization suggests the opening of K^+ channels. Conversely, the application of EPPTB to WT DA neurons was accompanied with a depolarization of the membrane potential to −35.8 ± 0.3 mV (n = 15), indicating that TAAR1 mediates an inhibitory tone.

DA neurons possess cation-permeable I_h channels that are activated by hyperpolarization and positively modulated by cAMP (13, 14). Therefore, a concomitant TAAR1-mediated hyperpolarization and increase in the intracellular cAMP concentration may support the activation of I_h currents. However, blocking I_h channels in WT mice with the inhibitor ZD7288 (20 μM) had no significant effect on the firing frequency in the presence or absence of *p*-tyr (control, 2.1 ± 0.8 Hz, n = 10; control+ZD7288, 2.2 ± 0.7 Hz, n = 5; *p*-tyr, 0.5 ± 0.1 Hz, n = 10; *p*-tyr + ZD7288, 0.4 ± 0.1 Hz, n = 5). This supports that I_h channels in DA neurons of the VTA are neither activated by TAAR1 nor involved in pacemaker frequency control, as already suggested by an earlier report (14).

EPPTB Inhibits a TAAR1-Induced G Protein-Dependent Outward Current in DA Neurons of the VTA. Voltage-clamp experiments revealed that at a physiological extracellular [K^+], bath application of *p*-tyr to DA neurons in the VTA induced an outward current with an EC_{50} value of 305 ± 11 nM, which agrees with EC_{50} values obtained at recombinant mouse receptors in other assays (Table 1 and Fig. S3). The outward current induced by *p*-tyr (10 μM) was associated with a 21% decrease of the apparent input resistance and inhibited by EPPTB (10 nM) (Fig. 3 *A* and *B*). In the presence of 1.5 nM EPPTB the *p*-tyr dose–response curve exhibited a parallel rightward shift with no significant reduction of the maximal response, consistent with the competitive mode of action of EPPTB (Fig. S3). It was proposed that trace amines cause an indirect activation of DA D2 receptors by enhancing the efflux of dopamine (12). However, the D2 antagonist sulpiride (10 μM) did not inhibit the *p*-tyr-induced current, showing that the current is not mediated by D2 receptors (Fig. 3*B*). Since TAAR1 is positively coupled to adenylate cyclase, we analyzed whether cAMP-dependent protein kinase A (PKA) modulates the *p*-tyr-induced outward current. In the presence of the PKA inhibitor H8 (10 μM), the amplitude of the outward current remained unchanged (Fig. 3*B*). Consistent with constitutive activity or tonic TAAR1 activation the holding current was reduced below baseline following EPPTB application. Neither *p*-tyr nor EPPTB had any effects on the holding current in *Taar1*$^{-/-}$ mice. In further support of constitutive or tonic TAAR1 activity, application of EPPTB in the absence of *p*-tyr elicited an apparent inward current in WT but not in *Taar1*$^{-/-}$ mice (Fig. 3 *C* and *D*). The EPPTB-induced inward current in WT neurons was associated with a 16% increase in input resistance, supporting the closure of K^+ channels. In WT mice, the EPPTB-induced inward current was significantly increased

Table 1. Comparison of binding affinities and EC_{50} values of p-tyr and EPPTB at human and rodent TAAR1

Compound	Parameter, assay, preparation	Mouse	Rat	Human
p-tyr	K_i, binding, HEK293*	404 ± 129	70 ± 12	nd
	EC_{50}, cAMP, HEK293†	545 ± 179	125 ± 36	1664 ± 135
	EC_{50}, GIRK, *Xenopus* oocytes‡§	167 ± 24	nd	nd
	EC_{50}, patch-clamp, VTA slices§	305 ± 11	nd	nd
EPPTB	K_i, binding, HEK293*	0.9 ± 0.1	942 ± 133	nd

*Radioligand [^{3}H]-rac-2-(1,2,3,4-tetrahydro-1-naphthyl)-2-imidazoline (12).
†Biotrak Enzyme Immunoassay for cAMP.
‡Current mediated by Kir3.1 and Kir3.2 co-expressed with TAAR1.
§Current at −50 mV holding potential; nd, not determined. Values are given as nM (mean ± SEM). The results were obtained from at least four independent experiments.

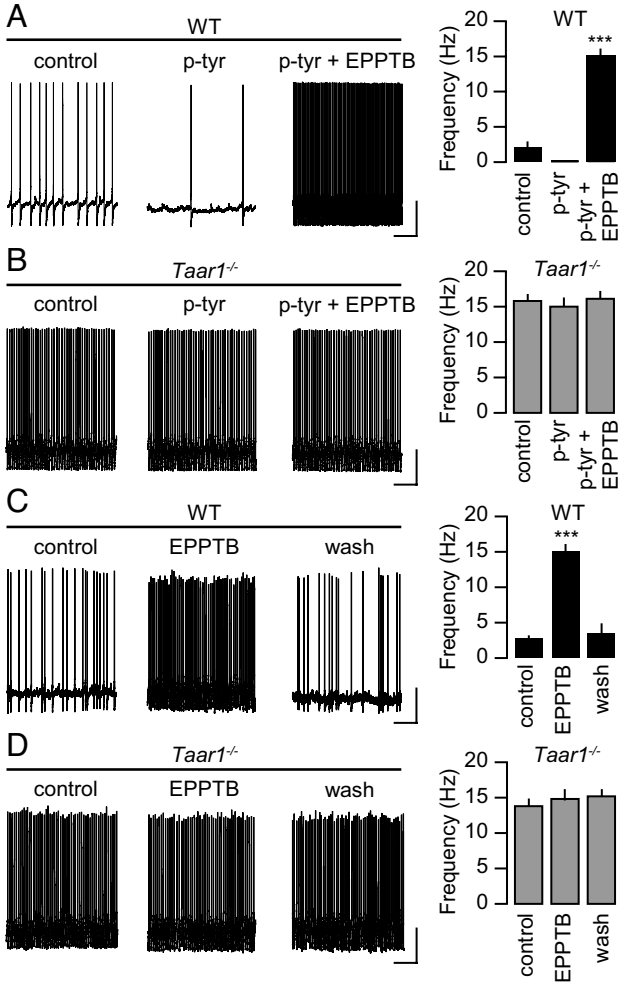

Fig. 2. Effects of *p*-tyr and EPPTB on the spontaneous firing rate of DA neurons in the VTA. (*A*) In neurons of WT mice, the firing frequency was assessed before (control) and during the application of *p*-tyr alone and in combination with EPPTB. EPPTB not only inhibited the *p*-tyr-mediated decrease in firing frequency but increased the firing frequency over control levels (control, 2.1 ± 0.8 Hz; *p*-tyr, 0.5 ± 0.1 Hz; *p*-tyr + EPPTB, 15.1 ± 1.0 Hz; $n = 10$; ***, $P < 0.001$ for *p*-tyr + EPPTB versus *p*-tyr). (*B*) In neurons of *Taar1*$^{-/-}$ mice the firing frequency was not significantly affected by application of *p*-tyr or EPPTB (control, 16.0 ± 1.0 Hz; *p*-tyr, 15.0 ± 1.3 Hz; *p*-tyr + EPPTB, 16.1 ± 1.1 Hz; $n = 10$). (*C*) In neurons of WT mice the firing frequency was significantly increased by EPPTB in the absence of *p*-tyr application. After wash-out of EPPTB for 1 h (wash) the firing frequency reverted close to control levels (control, 1.9 ± 0.2 Hz; EPPTB, 15.1 ± 1.0 Hz; wash, 3.5 ± 0.8 Hz; $n = 4$; ***, $P <$ 0.001 for EPPTB versus control). (*D*) In neurons of *Taar1*$^{-/-}$ mice, EPPTB had no effect on the firing frequency (control, 14.3 ± 1.1 Hz; EPPTB, 14.8 ± 0.9 Hz; wash, 15.2 ± 0.9 Hz; $n = 6$). In *A*–*D*, representative recordings are shown on the left and summary bar graphs on the right. (Scale bar, 20 mV/2 s.)

following preincubation of the slices with 100 μM pargyline (Fig. 3*D*), a nonspecific monoamine oxidase inhibitor increasing the extracellular TA concentration (15). TAAR1 may, similar to other GPCRs, gate Kir3-type K^+ channels via the $G_{\beta\gamma}$ subunits of the activated G protein (16). Consistent with this proposal, dialysis of DA neurons with GDPβS (2 mM for 40 min), a blocker of G protein activation, significantly reduced the *p*-tyr-mediated outward current (Fig. 3*E*).

Characterization of the *p*-tyr-Mediated Current in DA Neurons of the VTA. To determine whether the *p*-tyr-mediated current is carried by K^+ ions, we determined its current–voltage (I–V) relationship. We applied brief voltage ramps ranging from −20 to −140

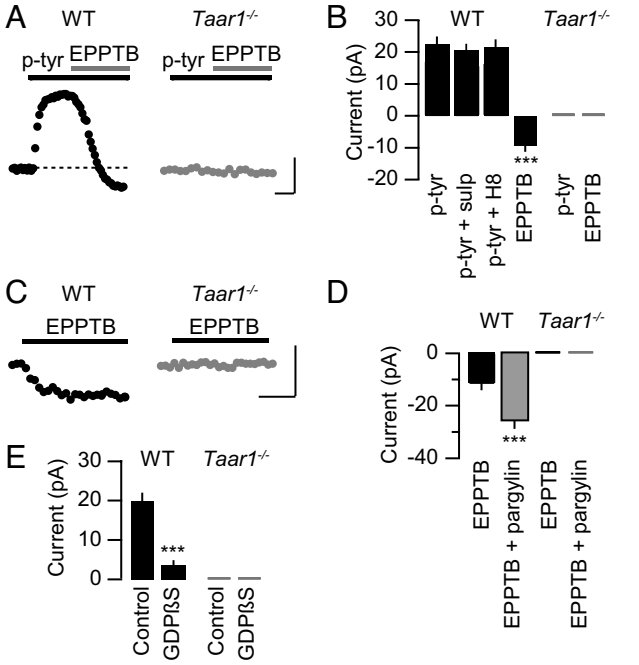

Fig. 3. TAAR1-evoked currents in DA neurons of the VTA. (*A*) Representative current traces recorded from DA neurons of WT (black trace) and *Taar1*$^{-/-}$ (gray trace) mice. Application of *p*-tyr (10 μM) induced an outward current in WT neurons that was antagonized by EPPTB (10 nM). (*B*) Summary bar graph illustrating that application of EPPTB reduced the current below baseline in WT but not in *Taar1*$^{-/-}$ neurons (WT: *p*-tyr, 21.2 ± 1.5 pA, EPPTB, −9.4 ± 0.6 pA; *Taar1*$^{-/-}$: *p*-tyr, 0.40 ± 0.01 pA, EPPTB, −0.05 ± 0.02 pA; $n = 7$, ***, $P <$ 0.001). The D2 antagonist sulpiride (sulp) did not significantly inhibit the outward current induced by *p*-tyr application (WT: *p*-tyr + sulp, 18.8 ± 0.8 pA, $n = 7$; $P > 0.05$ versus *p*-tyr). Likewise, infusion of the PKA inhibitor H8 via the recording pipette did not significantly alter the outward current induced by *p*-tyr (WT: *p*-tyr + H8, 20.7 ± 1.4, $n = 5$; $P > 0.05$ versus *p*-tyr). (*C*) Without preceding stimulation by *p*-tyr, EPPTB induced an apparent inward current in neurons from WT but not *Taar1*$^{-/-}$ mice. (*D*) Summary bar graph illustrating changes in the holding current following EPPTB application. The amplitude of the EPPTB-induced apparent inward current was significantly increased in the presence of the nonspecific monoamine oxidase inhibitor pargylin, which increases the extracellular TA concentration (WT: EPPTB, −11.5 ± 1.1 pA, EPPTB + pargylin, −25.9 ± 1.7 pA; *Taar1*$^{-/-}$: EPPTB, −0.04 ± 0.01 pA, EPPTB + pargylin, −0.15 ± 0.02 pA; $n = 5$; ***, $P < 0.001$). (*E*) Bar graph representing maximal *p*-tyr currents in the presence or absence of GDPβS (2 mM for 40 min), which was infused via the recording pipette (WT: control, 20.0 ± 1.0 pA; GDPβS, 3.6 ± 0.9 pA; *Taar1*$^{-/-}$: control, 0.10 ± 0.02 pA, GDPβS, 0.25 ± 0.01 pA; $n = 10$; ***, $P < 0.001$). [Scale bar, 5 min/10 pA in (*A*) and (*C*).]

mV in the absence and presence of *p*-tyr. The I–V relationship of the current induced by *p*-tyr was then calculated by subtracting the I–V curve in the absence of *p*-tyr from the I–V curve in the presence of *p*-tyr. In physiological extracellular $[K^+]$ the current induced by *p*-tyr showed inward rectification and reversed near the calculated K^+ equilibrium potential (2.5 mM $[K^+]_{ext}$, $V_{rev} = -101$ mV) (Fig. 4*A*). This supports that *p*-tyr selectively activates a K^+ current, further ruling out a contribution of a mixed Na^+/K^+ current from I_h channels (see above). In the presence of EPPTB a *p*-tyr-induced response was mostly lacking, similar to what is observed in *Taar1*$^{-/-}$ mice (Fig. 4*A*). The reversal potential of the *p*-tyr-induced current is shifted by rising the extracellular $[K^+]$ (12.5 mM $[K^+]_{ext}$, $V_{rev} = -60$ mV), confirming that the gating of K^+ channels underlies the *p*-tyr-induced current (Fig. 4*B*). The nonselective K^+ channel blocker Ba^{2+} (300 μM) and the Kir3 channel blocker tertiapin (10 μM) (17) occluded the *p*-tyr-induced current, suggesting that the activation of Kir3 channel underlies the K^+ current (Fig. S4).

PHARMACOLOGY

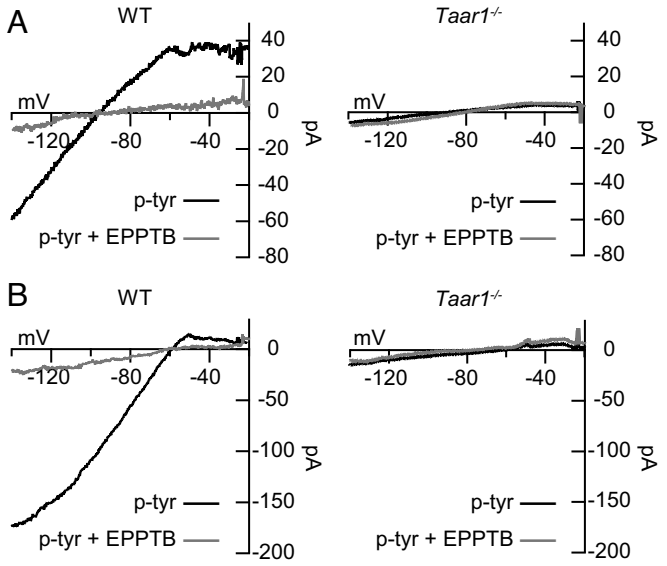

Fig. 4. TAAR1 activates an inwardly rectifying K^+ current in DA neurons of the VTA. The *p*-tyr-induced currents were obtained by calculating the difference between the I–V curves before and after addition of *p*-tyr (10 μM), both in the absence (black traces) and presence of EPPTB (10 nM, gray traces). (*A*) An inwardly rectifying, EPPTB-sensitive current was induced by *p*-tyr in neurons from WT but not *Taar1*$^{-/-}$ mice. At physiological extracellular [K^+] (2.5 mM) the polarity of the *p*-tyr-induced current reversed at −101 mV. (*B*) Raising extracellular [K^+] to 12.5 mM shifted the reversal potential of the *p*-tyr-induced current to −60 mV.

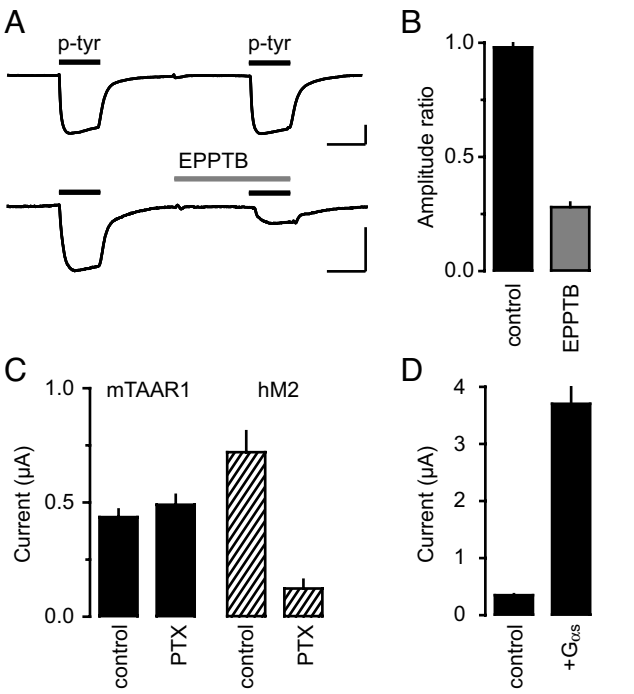

Fig. 5. TAAR1 activates Kir3 channels in *Xenopus* oocytes via PTX-insensitive G-proteins. (*A*) Current traces were recorded from oocytes clamped to −50 mV, which were injected with mRNAs encoding mouse TAAR1 and human Kir3.1/3.2. In the presence of 45 mM K^+ the application of *p*-tyr (10 μM, black bars) induced an inward current that was of similar amplitude with a second application of *p*-tyr (top trace). The *p*-tyr-induced current was reduced by EPPTB (bottom trace). (*B*) Bar graph depicting the ratio of the second-to-first *p*-tyr current response in the presence or absence of EPPTB (control). On average, EPPTB inhibited the *p*-tyr-induced current by 72 ± 2% ($n = 4$). (*C*) Bar graph depicting that PTX pretreatment did not significantly alter the *p*-tyr response of TAAR1 expressing oocytes. In contrast, PTX significantly reduced the response to acetylcholine (ACh, 10 μM) in oocytes expressing the human muscarinic ACh receptor 2 (hM2), which couples to Kir3 via $G_{i/o}$-type G-proteins. (*D*) Bar graph depicting the average amplitudes of oocytes injected with mRNAs for TAAR1 and Kir3.1/3.2 without (control) and with mRNA for human $G_{\alpha s}$ (20 pg/nL). Coexpression of $G_{\alpha s}$ drastically increased the *p*-tyr-mediated current. (Scale bar, 1 min/100 nA in *A*.)

TAAR1 Couples to Kir3 Channels in *Xenopus* Oocytes. To confirm that TAAR1 can activate Kir3 channels we coexpressed human Kir3.1 and Kir3.2 subunits together with mouse TAAR1 in *Xenopus* oocytes. At a holding potential of −50 mV and in the presence of elevated K^+ (45 mM) oocytes expressing Kir3 produced a tonic inward current, consistent with the reported constitutive activation of K^+ channels by excess free $G_{\beta\gamma}$ (18, 19). Application of *p*-tyr evoked an additional inward current (Fig. 5*A*). The EC_{50} of 167 nM for the *p*-tyr-induced current is comparable to the EC_{50} values measured in other assays (Table 1). The K^+-current in response to *p*-tyr (10 μM) was robustly reduced by EPPTB (3 μM) (Fig. 5 *A* and *B*). Intriguingly, EPPTB inhibited receptors heterologously expressed in *Xenopus* oocytes or HEK293 cells (cAMP assay) less potently than neuronal receptors. This may be attributable to differences in posttranslational receptor modifications or to interacting proteins allosterically influencing the antagonist binding-site. The *p*-tyr-induced current in *Xenopus* oocytes was not sensitive to pertussis toxin (PTX), supporting that the activation of Kir3 channels is mediated by G_s- and not by $G_{i/o}$-type G proteins (Fig. 5*C*). Accordingly, coexpression of the G protein subunit α_s increased the *p*-tyr-induced current (Fig. 5*D*), similarly as previously described for the β2-adrenergic receptor (19). No *p*-tyr-evoked current was seen in control oocytes injected with TAAR1 mRNA or Kir3.1/3.2 mRNA alone.

Increased Potency of DA at D2 Receptors in the Absence of TAAR1 Activity. *Taar1*$^{-/-}$ mice exhibit an increase in the high-affinity states of striatal D2 receptors (8), which is indicative of DA supersensitivity (20, 21). We therefore investigated whether acute blockade of TAAR1 activity modulates D2 receptors in DA neurons of the VTA. Bath application of the D2/D3 DA receptor agonist quinpirole (30 μM) induced an outward current that decreased during prolonged application (Fig. 6*A*). Preincubation of slices with EPPTB prevented this current desensitization. Likewise, DA neurons in *Taar1*$^{-/-}$ mice exhibited nondesensitizing, quinpirole-mediated currents, which were not altered in the presence of EPPTB (Fig. 6*B*). In the presence of the D2 receptor antagonist sulpiride (10 μM) the holding currents in WT slices preincubated with EPPTB were reduced below baseline (Fig. 6*A*). This suggests that D2 receptors become constitutively activated or tonically active in the absence of TAAR1 activity. Lack of TAAR1 activity not only correlates with a reduced desensitization rate and tonic or constitutive D2 receptor activity, but also with a simultaneous approximately 4-fold increase in agonist potency at D2 receptors (Fig. 6*C*). Of note, the potency of quinpirole at DA neurons in the presence of EPPTB was comparable to the potency of quinpirole at *Taar1*$^{-/-}$ DA neurons. In the presence of 40 nM *p*-tyr a parallel rightward shift of the quinpirole dose-response curve is observed, in support of TAAR1 activity reducing agonist potency at D2 receptors (Fig. 6*C*).

Discussion

To our knowledge, no other selective TAAR1 antagonist has been identified. EPPTB is more potent at mouse TAAR1 than at rat and human TAAR1. We characterized the pharmacological and physiological effects of EPPTB in the mouse brain, using *Taar1*$^{-/-}$ mice as a control. Trace amines such as *p*-tyr are known to reduce the firing frequency of DA neurons (7, 12, 22, 23).

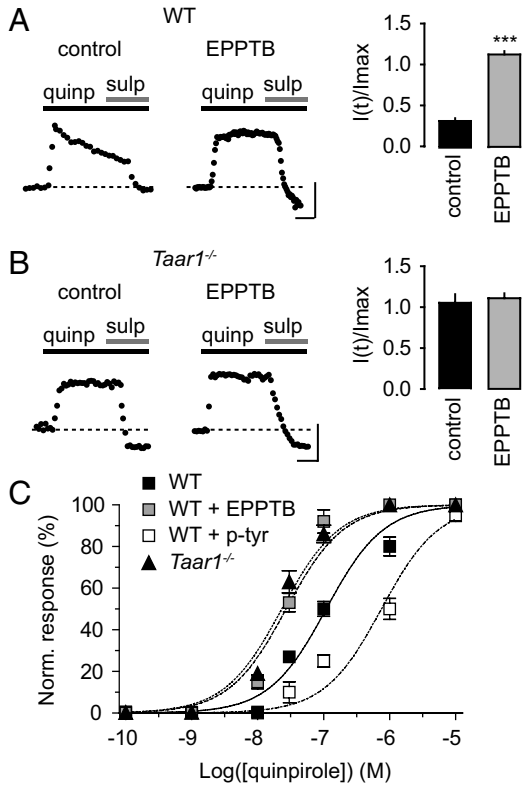

Fig. 6. TAAR1 activity modulates D2 receptor desensitization rate and agonist potency in DA neurons of the VTA. (*A* and *B*) Representative traces of quinpirole-induced currents in the presence and absence of EPPTB. (Scale bar, 5 min/20 pA.) Bar graphs represent the desensitization rate, which is expressed as the residual current after continuous quinpirole application for 15 min [I(t)], normalized to the initial maximal current (Imax). (*A*) Preincubation of WT slices with EPPTB (10 nM) prevents the D2 receptor desensitization seen in control slices (control, I(t)/Imax = 0.31 ± 0.04; EPPTB, I(t)/Imax = 1.08 ± 0.05; n = 9, ***, $P < 0.001$). (*B*) *Taar1*$^{-/-}$ slices exhibit non-desensitizing D2-mediated currents in the absence and presence of EPPTB (control, I(t)/Imax = 1.03 ± 0.14; EPPTB, I(t)/Imax = 1.09 ± 0.08; n = 6). Following application of the D2 antagonist sulpiride, the holding current was reduced below baseline (dotted line) in WT slices preincubated with EPPTB, similar as in *Taar1*$^{-/-}$ slices. (*C*) Dose-response relationships of the quinpirole-induced current in WT slices, WT slices preincubated with EPPTB (10 nM), WT slices preincubated with *p*-tyr (40 nM) and *Taar1*$^{-/-}$ slices. Current amplitudes were normalized to the maximal current obtained with a saturating concentration of quinpirole (10 μM). EC_{50} values: WT, 109.5 ± 3.8 nM, n = 9; WT + EPPTB, 27.2 ± 0.4 nM, n = 9; WT + *p*-tyr, 754.4 ± 6.6 nM, n = 4; *Taar1*$^{-/-}$, 23.3 ± 0.4 nM, n = 9.

Here, we show that in slices of the VTA, EPPTB antagonizes the *p*-tyr-mediated inhibition of DA neuron firing. In fact, incubation of VTA slices with EPPTB increases the spontaneous firing rate of DA neurons above the basal level, consistent with an increased firing rate of DA neurons observed in *Taar1* knockout mice (7). This corroborates the idea that TAAR1 normally exerts an inhibitory tone on DA neurons. We further show that activation of TAAR1 induces a G protein-dependent inwardly rectifying K^+ current that is inhibited by Ba^{2+} and tertiapin, suggesting that TAAR1 reduces the firing rate of DA neurons by activating Kir3 channels. It was proposed that trace amines cause an increased efflux of newly synthesized dopamine (12) that could activate a K^+ current via D2 receptors. However, pharmacological inhibition of D2 receptors with sulpiride does not inhibit the TAAR1-induced K^+ current, showing that the K^+ current is not triggered by D2 receptors. Instead, we found that in *Xenopus* oocytes TAAR1 directly activates Kir3 channels via PTX-insensitive G-proteins, most likely G_s proteins. This challenges an earlier report failing to demonstrate TAAR1 coupling to Kir3 channels (24). Our data reinforce that GPCRs coupled to G proteins other than $G_{i/o}$ can gate Kir3 channels (25–29). Federici and colleagues showed that the application of *p*-tyr to DA neurons at concentrations higher than those used in our study (at least 30 μM) attenuates $GABA_B$-mediated K^+ currents through a G protein-dependent process (30). While they did not study direct effects of TAAR1 on Kir3 channels, they suggested that a reduced coupling between $GABA_B$ receptors and Kir3 channels underlies this K^+ current attenuation. Possibly, low-affinity *p*-tyr receptors distinct from TAAR1 are involved in this uncoupling. However, since Kir3 current responses in DA neurons desensitize (31) it is also conceivable that a TAAR1-induced K^+-current desensitization contributes to the attenuation of the $GABA_B$ response.

We observed a functional link between TAAR1 and D2 receptors in DA neurons. Specifically, we found that the TAAR1 antagonist EPPTB increased agonist potency at D2 receptors while at the same time reducing their desensitization rate. A simultaneous increase in agonist potency and lack of desensitization makes D2 receptors ideally suited to sense ambient levels of DA. Presumably, this increases D2-mediated inhibition of DA neurons and balances the loss of TAAR1-mediated inhibition. The data support that TAAR1 is part of a homoeostatic regulatory mechanism that prevents excess activity of DA neurons. It is currently unknown by which molecular events TAAR1 influences D2 receptors. It is conceivable that TAAR1 regulates the phosphorylation state of D2 receptors, which may explain the rapid effects on D2 receptor pharmacology and kinetics after acute TAAR1 blockade with EPPTB.

It was proposed that TAAR1 inhibits locomotor activity via a downmodulation of DA neurotransmission (7). This is supported by our study demonstrating a TAAR1-mediated activation of K^+ channels in DA neurons. Because TAAR1 activates K^+ channels in DA tonically, the overruling effect of blocking TAAR1 is a net increase in the firing rate of DA neurons. Antagonizing TAAR1 with compounds like EPPTB may therefore potentially provide an approach to enhance the action of L-dopa in Parkinson's disease. Activating TAAR1, on the other hand, may be of therapeutic benefit in the treatment of schizophrenia, addiction, or attention deficit/hyperactivity disorder.

Materials and Methods

Generation of Cell Lines Stably Expressing TAAR1 and cAMP Measurements. Amplified genomic DNA was used to construct pIRESneo2 expression vectors encoding human, rat, and mouse TAAR1 (4). TAAR1 expressing cell lines were generated by transfecting HEK293 cells (ATCC) with expression plasmids using Lipofectamine 2000 (Invitrogen). Cells were cultured for 10 days in the presence of 1 mg/mL G418 (Sigma). Individual colonies were expanded and tested for responsiveness to TAs (Sigma) using the cAMP Biotrak Enzyme Immunoassay (EIA).

Membrane Preparation and Radioligand Binding. Cells were rinsed with ice-cold PBS (without Ca^{2+} and Mg^{2+}) containing 10 mM EDTA and pelleted at 1,000 rpm for 5 min at 4 °C. The pellet was washed twice with ice-cold PBS, frozen in liquid nitrogen, and stored at −80 °C. Frozen pellets were suspended in 20 mL HEPES-NaOH (20 mM, pH 7.4) containing 10 mM EDTA and homogenized with a Polytron (PT 3000, Kinematica) at 10,000 rpm for 10 s. The homogenate was centrifuged at 48,000 × *g* for 30 min at 4 °C and the pellet suspended in 20 mL HEPES-NaOH containing 0.1 mM EDTA (buffer A). This procedure was repeated twice, the final pellet resuspended at 200 μg protein per mL in HEPES-NaOH (20 mM, pH 7.0) containing $MgCl_2$ (10 mM) and $CaCl_2$ (2 mM) (buffer B) and homogenized with a Polytron at 10,000 rpm for 10 s. Binding assays were performed for 30 min at 4 °C in a final volume of 1 mL. The TAAR1 radioligand [^{3}H]-rac-2-(1,2,3,4-tetrahydro-1-naphthyl)-2-imidazoline (11) was used at a concentration equal to the calculated K_d value of 60 nM, which resulted in the binding of approximately 0.1% of the radioligand and a specific binding representing approximately 70–80% of the total binding. Nonspecific binding was defined as the amount of [^{3}H]-rac-2-(1,2,3,4-tetrahydro-1-naphthyl)-2-imidazoline bound in the presence of 10 μM unla-

PHARMACOLOGY

belled ligand. All compounds were tested at a broad range of concentrations (10 pM to 10 μM) in duplicate. Incubations were terminated by rapid filtration through UniFilter-96 plates (Packard Instrument Company) and glass filters GF/C presoaked for at least 2 h in polyethylenimine 0.3%. Tubes and filters were washed three times with 1 mL of cold buffer B. Wet filters were soaked in Ultima gold (45 μL/well) and the radioactivity counted using a TopCount Microplate Scintillation Counter (Packard Instrument Company).

Electrophysiology in Brain Slices. Horizontal slices (250-μm) of the midbrain were made from adult mice (3–6 months of age) in cooled artificial cerebrospinal fluid containing (in mM): NaCl 119, KCl 2.5, $MgCl_2$ 1.3, $CaCl_2$ 2.5, NaH_2PO_4 1.0, $NaHCO_3$ 26.2, and glucose 11, bubbled with 95% O_2 and 5% CO_2. After 1 h slices were transferred to the recording chamber and superfused with 1.5 mL min^{-1} artificial cerebrospinal fluid. Visual whole-cell voltage-clamp or current-clamp recording techniques were used to measure holding currents of DA neurons at −50 mV or to record spontaneous spiking activity, respectively. DA cells were identified by their large I_h current and an outward current in response to the D2 receptor agonist quinpirole (10 μM). The internal solution contained (in mM): potassium gluconate 130, $MgCl_2$ 4, EGTA 1.1, HEPES 5, Na_2ATP 3.4, sodium creatine-phosphate 10, and Na_3GTP 0.1. Signals were amplified, filtered at 1 kHz (Axopatch 200B), digitized at 5 kHz (Digidata 1322A card) and saved on hard disk (pClamp9, Axon Instruments). Current-voltage (I–V) relationships were determined by ramp-command protocols (from −20 to −140 mV, 250 ms duration) in the presence of TEA and 4-AP in the external solution (32). Data are presented as mean ± SEM. For statistical comparison of two groups the nonparametric Mann-Whitney test was used (GraphPad InStat 3.0). For statistical comparison of multiple groups two-way ANOVA was used. For statistical comparison of frequencies the Kolmogorov-Smirnov test was used. Quinpirole, sulpiride, ZD7288, and *p*-tyr were from Sigma.

Electrophysiology in *Xenopus* Oocytes. Plasmids encoding mouse TAAR1 and human Kir3.1/3.2 were linearized, mRNA synthesized (mMESSAGE mMACHINE Ultra, Ambion) and mRNA purified (MEGAclear kit, Ambion). Capped and polyA tailed mRNA was microinjected into *Xenopus laevis* oocytes (EcoCyte Bioscience). Each oocyte was injected with 50 nL of an aqueous solution containing 20 pg/nL mouse TAAR1 mRNA and 0.5 pg/nL Kir3.1 and Kir3.2 mRNA. The Roboocyte instrument (Multi Channel Systems) was used for oocyte injection and voltage-clamp experiments. Experiments were performed 4–6 days after mRNA injection. During electrical recording the oocytes were constantly superfused with a solution containing (in mM): NaCl 46, KCl 45, $MgCl_2$ 1, $CaCl_2$ 1, HEPES 5, pH adjusted to 7.4 by addition of NaOH. In some experiments PTX (≈5 ng/oocyte, Sigma) was injected into the oocytes 2 days before recording. Quantitative data are presented as mean ± SEM. The *t*-test was used for statistical comparison.

ACKNOWLEDGMENTS. We thank S. Chaboz, V. Metzler, P. Biry, P. Pflimlin, and V. Graf for technical assistance and R. Seddik and R. Turecek for comments on the manuscript. This work was supported by F. Hoffmann-La Roche Ltd, Swiss Science Foundation Grant 3100A0-117816 (to B.B.) and European Community's Seventh Framework Program Grant FP7/2007-2013 under Grant Agreement 201714.

1. Berry MD (2004) Mammalian central nervous system trace amines. Pharmacologic amphetamines, physiologic neuromodulators. *J Neurochem* 90:257–271.
2. Borowsky B, et al. (2001) Trace amines: Identification of a family of mammalian G protein-coupled receptors. *Proc Natl Acad Sci USA* 98:8966–8971.
3. Bunzow JR, et al. (2001) Amphetamine, 3,4-methylenedioxymethamphetamine, lysergic acid diethylamide, and metabolites of the catecholamine neurotransmitters are agonists of a rat trace amine receptor. *Mol Pharmacol* 60:1181–1188.
4. Lindemann L, et al. (2005) Trace amine-associated receptors form structurally and functionally distinct subfamilies of novel G protein-coupled receptors. *Genomics* 85:372–385.
5. Lindemann L, Hoener MC (2005) A renaissance in trace amines inspired by a novel GPCR family. *Trends Pharmacol Sci* 26:274–281.
6. Burchett SA, Hicks TP (2006) The mysterious trace amines: Protean neuromodulators of synaptic transmission in mammalian brain. *Prog Neurobiol* 79:223–246.
7. Lindemann L, et al. (2008) Trace amine-associated receptor 1 modulates dopaminergic activity. *J Pharmacol Exp Ther* 324:948–956.
8. Wolinsky TD, et al. (2007) The Trace Amine 1 receptor knockout mouse: An animal model with relevance to schizophrenia. *Genes Brain Behav* 6:628–639.
9. Berry MD (2007) The potential of trace amines and their receptors for treating neurological and psychiatric diseases. *Rev Recent Clin Trials* 2:3–19.
10. Sotnikova TD, Zorina OI, Ghisi V, Caron MG, Gainetdinov RR (2008) Trace amine associated receptor 1 and movement control. *Parkinsonism Relat Disord* 14(Suppl 2):S99–102.
11. Galley G, Zbinden KG, Norcross R, Stalder H (2009) Benzamide derivatives and their use for treating CNS disorders. *International Patent Application* WO2009016088.
12. Geracitano R, Federici M, Prisco S, Bernardi G, Mercuri NB (2004) Inhibitory effects of trace amines on rat midbrain dopaminergic neurons. *Neuropharmacology* 46:807–814.
13. Lacey MG, Mercuri NB, North RA (1989) Two cell types in rat substantia nigra zona compacta distinguished by membrane properties and the actions of dopamine and opioids. *J Neurosci* 9:1233–1241.
14. Neuhoff H, Neu A, Liss B, Roeper J (2002) I(h) channels contribute to the different functional properties of identified dopaminergic subpopulations in the midbrain. *J Neurosci* 22:1290–1302.
15. Grimsby J, et al. (1997) Increased stress response and beta-phenylethylamine in MAOB-deficient mice. *Nat Genet* 17:206–210.
16. Mark MD, Herlitze S (2000) G-protein mediated gating of inward-rectifier K+ channels. *Eur J Biochem* 267:5830–5836.
17. Jin W, Lu Z (1998) A novel high-affinity inhibitor for inward-rectifier K+ channels. *Biochemistry* 37:13291–13299.
18. Herlitze S, Ruppersberg JP, Mark MD (1999) New roles for RGS2, 5 and 8 on the ratio-dependent modulation of recombinant GIRK channels expressed in Xenopus oocytes. *J Physiol* 517(Pt 2):341–352.
19. Lim NF, Dascal N, Labarca C, Davidson N, Lester HA (1995) A G protein-gated K channel is activated via beta 2-adrenergic receptors and G beta gamma subunits in Xenopus oocytes. *J Gen Physiol* 105:421–439.
20. Seeman P, et al. (2006) Psychosis pathways converge via D2high dopamine receptors. *Synapse* 60:319–346.
21. Seeman P, et al. (2005) Dopamine supersensitivity correlates with D2High states, implying many paths to psychosis. *Proc Natl Acad Sci USA* 102:3513–3518.
22. Rodriguez M, Barroso N (1995) beta-Phenylethylamine regulation of dopaminergic nigrostriatal cell activity. *Brain Res* 703:201–204.
23. Pinnock RD (1983) Sensitivity of compacta neurones in the rat substantia nigra slice to dopamine agonists. *Eur J Pharmacol* 96:269–276.
24. Regard JB, et al. (2007) Probing cell type-specific functions of Gi in vivo identifies GPCR regulators of insulin secretion. *J Clin Invest* 117:4034–4043.
25. Dascal N (1997) Signalling via the G protein-activated K^+ channels. *Cell Signal* 9:551–573.
26. Wickman K, Clapham DE (1995) Ion channel regulation by G proteins. *Physiol Rev* 75:865–885.
27. Robillard L, Ethier N, Lachance M, Hebert TE (2000) Gbetagamma subunit combinations differentially modulate receptor and effector coupling in vivo. *Cell Signal* 12:673–682.
28. Wickman KD, et al. (1994) Recombinant G-protein beta gamma-subunits activate the muscarinic-gated atrial potassium channel. *Nature* 368:255–257.
29. Wellner-Kienitz MC, Bender K, Pott L (2001) Overexpression of beta 1 and beta 2 adrenergic receptors in rat atrial myocytes. Differential coupling to G protein-gated inward rectifier K^+ channels via G_s and $G_{i/o}$. *J Biol Chem* 276:37347–37354.
30. Federici M, et al. (2005) Trace amines depress GABA B response in dopaminergic neurons by inhibiting G-betagamma-gated inwardly rectifying potassium channels. *Mol Pharmacol* 67:1283–1290.
31. Cruz HG, et al. (2004) Bi-directional effects of $GABA_B$ receptor agonists on the mesolimbic dopamine system. *Nat Neurosci* 7:153–159.
32. Lesage F (2003) Pharmacology of neuronal background potassium channels. *Neuropharmacology* 44:1–7.